ELECTRIC POWER
RESEARCH INSTITUTE

Kinetics and Morphology of Oxide Formed on Fe-9Cr-1Mo (Grade 91)

1017470

Kinetics and Morphology of Oxide Formed on Fe-9Cr-1Mo (Grade 91)

1017470

Technical Update, November 2009

EPRI Project Manager

K. Coleman

ELECTRIC POWER RESEARCH INSTITUTE
3420 Hillview Avenue, Palo Alto, California 94304-1338 ▪ PO Box 10412, Palo Alto, California 94303-0813 ▪ USA
800.313.3774 ▪ 650.855.2121 ▪ askepri@epri.com ▪ www.epri.com

DISCLAIMER OF WARRANTIES AND LIMITATION OF LIABILITIES

THIS DOCUMENT WAS PREPARED BY THE ORGANIZATION(S) NAMED BELOW AS AN ACCOUNT OF WORK SPONSORED OR COSPONSORED BY THE ELECTRIC POWER RESEARCH INSTITUTE, INC. (EPRI). NEITHER EPRI, ANY MEMBER OF EPRI, ANY COSPONSOR, THE ORGANIZATION(S) BELOW, NOR ANY PERSON ACTING ON BEHALF OF ANY OF THEM:

(A) MAKES ANY WARRANTY OR REPRESENTATION WHATSOEVER, EXPRESS OR IMPLIED, (I) WITH RESPECT TO THE USE OF ANY INFORMATION, APPARATUS, METHOD, PROCESS, OR SIMILAR ITEM DISCLOSED IN THIS DOCUMENT, INCLUDING MERCHANTABILITY AND FITNESS FOR A PARTICULAR PURPOSE, OR (II) THAT SUCH USE DOES NOT INFRINGE ON OR INTERFERE WITH PRIVATELY OWNED RIGHTS, INCLUDING ANY PARTY'S INTELLECTUAL PROPERTY, OR (III) THAT THIS DOCUMENT IS SUITABLE TO ANY PARTICULAR USER'S CIRCUMSTANCE; OR

(B) ASSUMES RESPONSIBILITY FOR ANY DAMAGES OR OTHER LIABILITY WHATSOEVER (INCLUDING ANY CONSEQUENTIAL DAMAGES, EVEN IF EPRI OR ANY EPRI REPRESENTATIVE HAS BEEN ADVISED OF THE POSSIBILITY OF SUCH DAMAGES) RESULTING FROM YOUR SELECTION OR USE OF THIS DOCUMENT OR ANY INFORMATION, APPARATUS, METHOD, PROCESS, OR SIMILAR ITEM DISCLOSED IN THIS DOCUMENT.

ORGANIZATION(S) THAT PREPARED THIS DOCUMENT

Oak Ridge National Laboratory (ORNL)

This is an EPRI Technical Update report. A Technical Update report is intended as an informal report of continuing research, a meeting, or a topical study. It is not a final EPRI technical report.

NOTE

For further information about EPRI, call the EPRI Customer Assistance Center at 800.313.3774 or e-mail askepri@epri.com.

Electric Power Research Institute, EPRI, and TOGETHER…SHAPING THE FUTURE OF ELECTRICITY are registered service marks of the Electric Power Research Institute, Inc.

Copyright © 2009 Electric Power Research Institute, Inc. All rights reserved.

CITATIONS

This document was prepared by

Oak Ridge National Laboratory
Corrosion Science and Technology Group
Materials Science and Technology Division
Oak Ridge, TN 37831

Principal Investigators
B. A. Pint
I. G. Wright

Electric Power Research Institute (EPRI)
Nondestructive Evaluation (NDE) Program
1300 W.T. Harris Blvd.
Charlotte, NC 28262

This document describes research sponsored by Electric Power Research Institute (EPRI).

This publication is a corporate document that should be cited in the literature in the following manner:

Kinetics and Morphology of Oxide Formed on Fe-9Cr-1Mo (Grade 91). EPRI, Palo Alto, CA: 2009. 1017470.

PRODUCT DESCRIPTION

Around the world, new coal-fired power plants with steam conditions hotter than those found in most U.S. plants have been making extensive use of Fe-9Cr-1Mo (Grade 91) ferritic/martensitic steel. For the hottest tubes, austenitic steels TP347HFG and Super 304H are the typical choices. The superior high-temperature creep strength of Grade 91 alloy (compared to earlier ferritic steels) allows thinner-walled tubes to be used at the higher temperatures, resulting in lower cost and better mechanical performance. However, failures have been experienced in recent years in tubes and piping made from the alloy in heat recovery steam generators in gas turbine combined-cycle service and in superheater/reheater tubes in coal-fired boilers. Some of these failures occurred as soon as two years after plant installation.

A broad survey of the problems experienced by the electric utility industry with the Grade 91 alloy was presented in the Electric Power Research Institute (EPRI) report *Service Experience with Grade 91 Components* (1018151). The narrower focus of the present report is practical research conducted by EPRI and Oak Ridge National Laboratory (ORNL) into the oxidation behavior of Grade 91 alloy steel after it has been exposed to dry air or steam.

Results and Findings

This report includes kinetic and morphology data for Grade 91 ferritic/martensitic steel exposed in dry air at 1 bar (15 psi) at 750–1100°C (1382–2012°F) and in steam at 17 bar (247 psi) at 600°C (1112°F). The steam data include the effect of pre-oxidation in air on the mass gain and scale morphology for 1-kh steam exposures. A pre-oxidation at 750°C (1382°F) appeared to be beneficial after 1 kh, but it probably would not produce a long-term benefit. Thicker oxides pre-formed at high temperature did not appear to be beneficial. The data provided in this report might provide a basis for comparing field-heat-treated Grade 91 welds to determine the heat treatment temperature based on the oxide thickness.

Overall, normalizing (1 h at 1050°C) and tempering (2 h at 750°C) heat treatments of Grade 91 in air produce oxide scales that are sufficiently thick (and/or inherently non-adherent) that they will be lost by spallation when those surfaces are exposed to steam. The techniques used in the study that is the subject of this report did not permit a reliable estimation of the amount or size of the spalled oxide. Nevertheless, such scale spallation carries the potential for problems in service.

The report suggests that minimizing scale formation by controlling the environment or removing the pre-oxidized scale before exposure to steam are desirable strategies. These strategies would be easier to implement for shop-fabricated parts than field repairs. In the field, perhaps reducing the normalizing temperature to near ~1000°C (-1768°F) and minimizing the normalizing time could reduce the amount of oxidation.

Challenges and Objectives

Failures in Grade 91 steel have resulted in serious consequences, including fatalities. Entirely different root causes for such failures are possible. One school of thought is that failure is caused by overheating and loss of strength of the tubes in service due to 1) blockage of the steam flow by the accumulation of exfoliated oxide scale at tube bends or 2) the steam-side scale lifting but not exfoliating. The second theory is that failure is caused by a reduction in strength resulting from improper heat treatment of the tubes, which could occur during shop fabrication or following welding in the field or fabrication shop. Correct identification of the root cause or causes is a prerequisite to implementation of effective permanent solutions.

Applications, Value, and Use

This report will be valuable to utility engineers and managers who are charged with operating plants that contain components fabricated with Grade 91 alloy. Photographs and light microscopy images of treated specimens and analysis of them will help personnel better understand the mechanisms involved in Grade 91 steel failures.

EPRI Perspective

EPRI and ORNL undertook this research for the benefit of EPRI-member utilities and other industries that use Grade 91 steel in high-temperature applications. The goal is to help utilities continue to use Grade 91 tubes and piping—which offer better performance at a lower cost—while reducing or eliminating the occurrence of operational defects and improving worker safety. Section 5 of the report contains recommendations for future research.

Approach

The objectives of this project were to provide a more complete data set on the oxidation behavior of Grade 91 and to determine the effect of pre-oxidation in air at higher temperatures on subsequent steam oxidation at 600°C (1112°F). Coupons of Grade 91 steel were machined from a commercial heat with composition of Fe-8.3Cr-0.9Mo-0.34Mn-0.26V-0.13Si-0.13Ni-0.079C-0.054N-0.001S as determined by inductively coupled plasma and combustion analysis. Coupons were polished to a 600-grit finish, ultrasonically cleaned, and weighed on a Mettler-Toledo AG265 microbalance. Isothermal mass gain was measured using a Cahn Model 1000 microbalance in dry, flowing air at 750–1100°C (1382–2012°F) in 50°C increments for times from 1 h to 10 h. Exposures in steam were conducted at 600°C (1112°F) in a high-pressure test rig at ORNL. Specimens were either as-polished or pre-oxidized in dry air.

After exposure in air or steam, the specimens were weighed and selected specimens were examined using X-ray diffraction, a scanning electron microscope equipped with energy dispersive X-ray analysis, and electron microprobe analysis equipped with wavelength dispersive X-ray analysis. The specimens were copper plated and metallographically sectioned to examine the reaction product in cross section.

Keywords

Failure analysis
Ferritic/martensitic steel
Grade 91 steel
Oxidation
Oxide scale
Spalling

CONTENTS

1

INTRODUCTION

In recent years, new coal-fired power plants have been installed around the world with steam conditions somewhat higher than those in U.S. plants. These units make extensive use of Grade 91 ferritic/martensitic steel (Fe-9Cr-1Mo), typically with austenitic steels TP347HFG and Super 304H used for the hottest tubes. The superior high-temperature creep strength of Grade 91 steel (compared with earlier ferritic steels) allows thinner walled tubes to be used at higher temperatures, resulting in lower cost and better mechanical performance. However, failures have been experienced in recent years in tubes and piping made from Grade 91 steel, in heat-recovery steam generators in gas turbine-combined cycle service, and in superheater/reheater tubes in coal-fired boilers after times as short as two years since the new tubing was installed. Some failures have resulted in serious consequences, including fatalities.

There are two schools of thought concerning the causes of these tube failures:

1. Overheating and loss of tube strength in service due to blockage of the steam flow by the accumulation of exfoliated oxide scale at tube bends, which would be expected to result in general overheating of the blocked tube run, or due to the steam-side scale lifting but not exfoliating, which would be expected to lead to localized overheating
2. Reduction in strength due to improper heat treatment of the tubes, which could occur during shop fabrication or after welding in the field or in the fabrication shop

These two scenarios suggest entirely different root causes for such failures; therefore, it is critically important that the root cause(s) are correctly identified before permanent solutions can be devised and implemented.

The goal of this project was to provide a more complete data set on the oxidation behavior of Grade 91 and to determine the effect of pre-oxidation in air at higher temperatures on subsequent steam oxidation at 600°C (1112°F). Thermogravimetric analysis (TGA) was used to measure the isothermal oxidation rate of Grade 91 in dry air at 750°C–1100°C (1382°F–2012°F). The specimens were then sectioned to examine the oxide thickness, structure, and composition in selected cases. In order to determine the effect of pre-oxidation on subsequent steam oxidation, Grade 91 specimens were pre-oxidized in dry air before exposure to steam at 17 bar (247 psi). The pre-oxidation conditions were intended to duplicate those associated with the normalizing (for example, 1 hour at 1050°C [1922°F]) and tempering (for example, 2 hours at 750°C [1382°F]) heat treatments applied to Grade 91 before service or to welds after tube repair.

2

EXPERIMENTAL PROCEDURE

Coupons of Grade 91 (~1.5 x 10 x 19 mm) were electrodischarge-machined (EDM) from a commercial heat with composition of Fe-8.3Cr-0.9Mo-0.34Mn-0.26V-0.13Si-0.13Ni-0.079C-0.054N-0.001S as determined by inductively coupled plasma (ICP) and combustion analysis. Coupons were polished to a 600-grit finish and ultrasonically cleaned and weighed using a Mettler-Toledo AG265 microbalance. Isothermal mass gain was measured using a Cahn model 1000 microbalance in dry, flowing air at 750°C–1100°C (1382°F–2012°F) in 50°C (122°F) increments from 1 to 10 hours. Exposures in steam were conducted at 600°C (1112°F) in a high-pressure test rig at ORNL. Specimens were either as-polished or pre-oxidized in dry air.

After exposure in air or steam, the specimens were weighed, and selected specimens were examined using X-ray diffraction (XRD), a scanning electron microscope (SEM) equipped with energy dispersive X-ray analysis, and an electron microprobe analysis (EPMA) machine equipped with wavelength dispersive X-ray analysis. Specimens were Cu plated and metallographically sectioned to examine the reaction product in the cross section.

3

RESULTS AND DISCUSSION

Oxidation in Dry Air: Kinetics

Figure 3-1 gives an example of some of the continuously measured TGA mass-gain data for Grade 91 coupons in dry air. The mass gain was plotted versus the square root of time to determine if there was a parabolic relationship. The mass gain was very high, particularly at higher temperatures, and there was an increase in rate after ~1 hour, such that the kinetic behavior could be represented by two parabolic rate constants: one rate from a 1-hour exposure and a second rate from a 10-hour exposure. These values are shown in Figure 3-2.

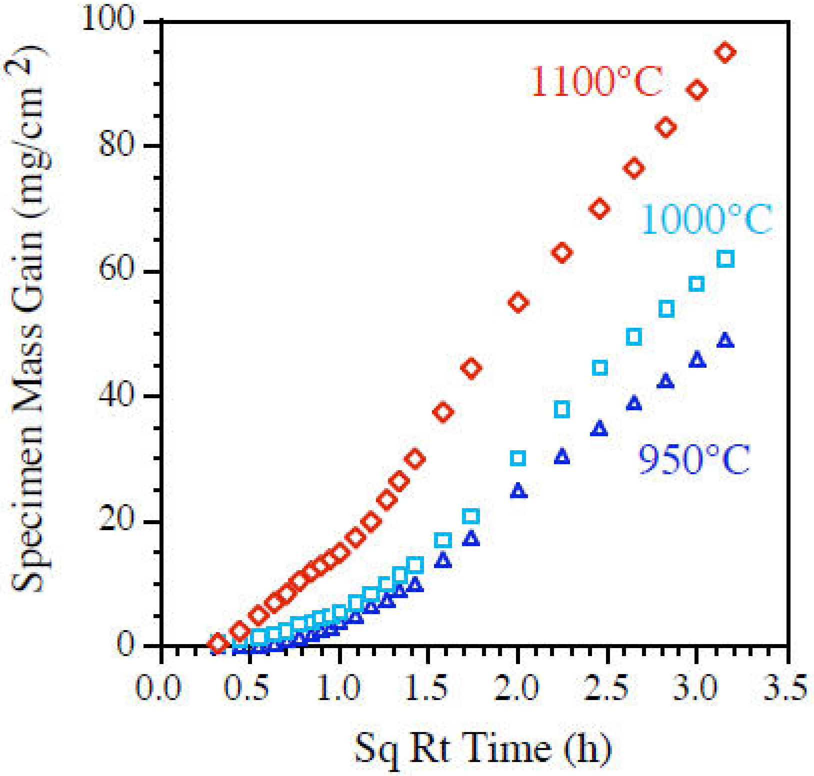

Figure 3-1
Specimen mass gain of Grade 91 specimens exposed in dry air measured using thermogravimetric analysis

The Arrhenius-type plot in Figure 3-2 indicates that the oxidation rates follow the expected temperature relationship, particularly for the lower temperatures from 750°C–950°C (1382°F–1742°F). Between 950° (1742°F) and 1100°C (2012°F), the calculated rates do not increase significantly with temperature. Those rates were extremely high with a significant amount of the 1.5-mm section consumed (as shown in later figures).

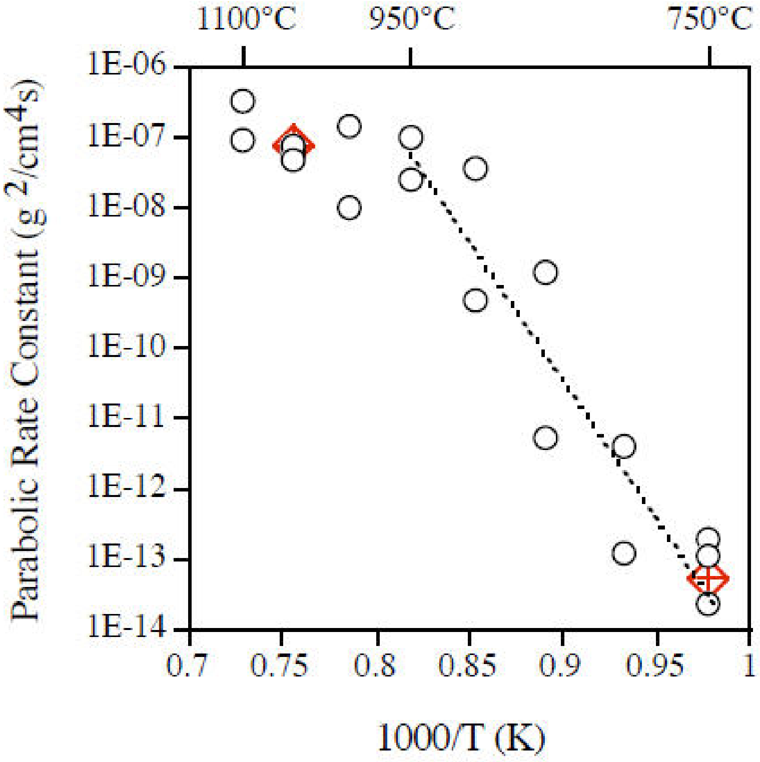

Figure 3-2.
Arrhenius plot of the parabolic rate constants for each of the exposures of Grade 91 in dry air from 750°C–1100°C (1382°F–2012°F). The lower rate at each temperature is for the shorter exposure time (1 hour), while the higher rate is for the 10-hour exposure. The rates from 750°C–950°C (1382°F–1742°F) follow one activation energy (dashed line), while the higher temperatures show only a minor increase in rate with temperature. The diamonds are the rate constant determined by the final mass change data shown in Figure 3-3b.

The final specimen mass gains measured after exposure and cooling to room temperature are shown in Figure 3-3 and compared with the total mass gain determined by TGA. Most of the TGA and final mass gains are in good agreement; however, there was obvious spallation of thicker oxides for some specimens (for example, 1 h at 1000°C [1832°F] and 10 h at 1050°C [1922°F]). The 10-hour, 1050°C (1922°F) TGA mass gain was not consistent with the other temperatures, and the 10-hour exposure at 1050°C (1922°F) should be repeated. Comparing the 1-hour and 10-hour data in Figure 3-3a, an accelerated oxidation rate was observed at 850°C (1562°F) and higher temperatures for the 10-hour exposures. Accelerated oxidation after 1 hour of exposure was observed at 950°C (1742°F) and higher temperatures. Protective behavior at the lower temperature and shorter times was attributed to the initial formation of a protective Cr-rich surface oxide or scale. With only ~9%Cr in Grade 91, the Cr likely became depleted in the alloy during exposure at 850°C (1562°F) and 900°C (1652°F), leading to faster growing, Fe-rich oxide formation. In Figure 3-3b, final and TGA mass gains are shown at 1050°C (1922°F) and 750°C (1382°F) versus the square root of time for exposures of 1, 2, 5, and 10 hours. At 1050°C (1922°F), the difference between the TGA and final mass gain after cooling to room temperature indicated significant spallation for most of the specimens. The linear relationship in this plot indicated parabolic kinetics at both temperatures, and the rates from these lines are shown as diamonds in Figure 3-2.

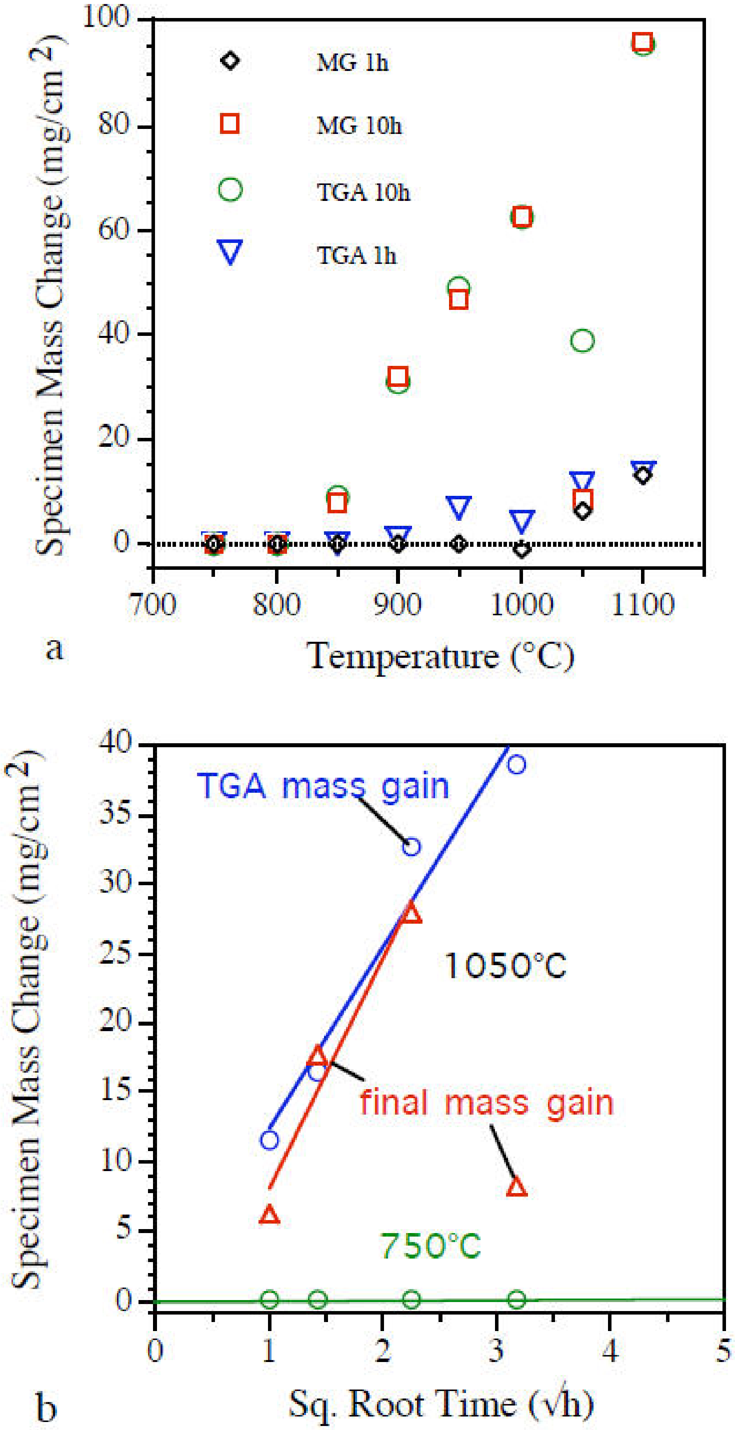

Figure 3-3
Mass change of Grade 91 specimens exposed in dry air after cooling to room temperature: (a) plot of the 1- and 10-hour TGA and final mass gain data as a function of exposure temperature and (b) mass change at 750°C (1382°F) and 1050°C (1922°F) as a function of the square root of time. Beginning at 850°C (1562°F), thicker oxides began to form as noted by the large mass change of the 10-hour specimen compared with the low mass gain (thin oxide) formed after 1 hour. Oxide spallation can significantly alter the specimen mass change after cooling.

Oxide Morphology

Figure 3-4 shows the polished cross section of the specimens exposed at 1000°C–1100°C (1832°F–2012°F). At 1100°C (1832°F), most of the oxide spalled on cooling. The oxide was extremely thick, as shown by the consumption of ~50% of the Grade 91 cross section after 10 hours in Figure 3-4b.

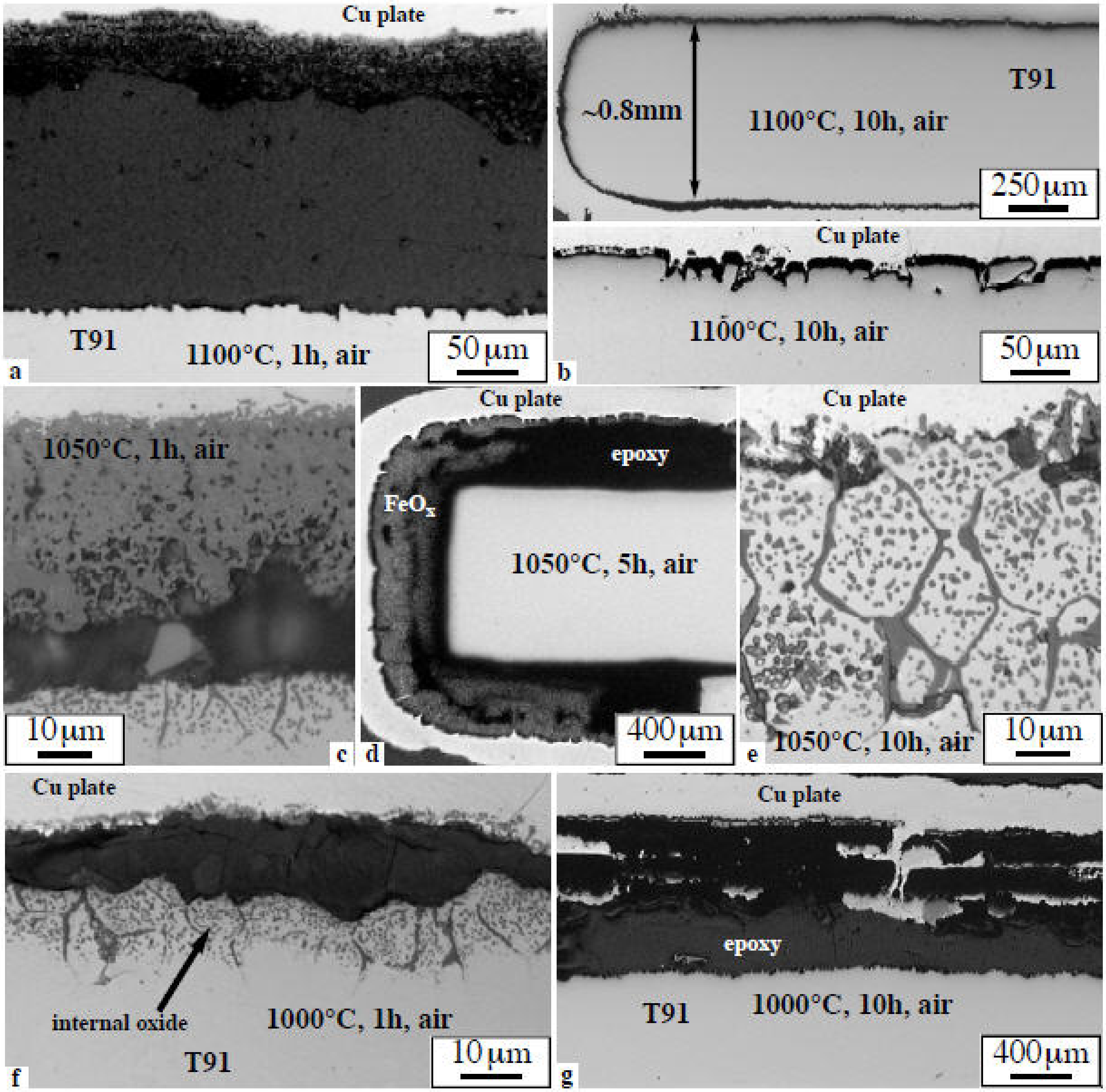

Figure 3-4
Light microscopy of polished Grade 91 specimens exposed in dry, flowing air for (a) 1 hour at 1100°C (2012°F), (b) 10 hours at 1100°C (2012°F), (c) 1 hour at 1050°C (1922°F), (d) 5 hours at 1050°C (1922°F), (e) 10 hours at 1050°C (1922°F), (f) 1 hour at 1000°C (1832°F), and (g) 10 hours at 1000°C (1832°)

At higher magnification, only a rough metal interface remained with little internal oxidation. At 1000°C (1832°F) and 1050°C (1922°F), the thick oxide also tended to spall; however, in some locations, the full-scale thickness was retained, such as after 5 hours at 1050°C (1922°F) in Figure 3-4d. At the higher magnifications, internal oxidation was evident (Figures 3-4e and 3-4f) and increased with exposure time and temperature. In Figure 3-4g, only loose pieces of oxide remained. The EPMA maps in Figure 3-5 indicate that the internal oxidation is the result of forming Cr_2O_3 in the metal rather than in a continuous surface layer.

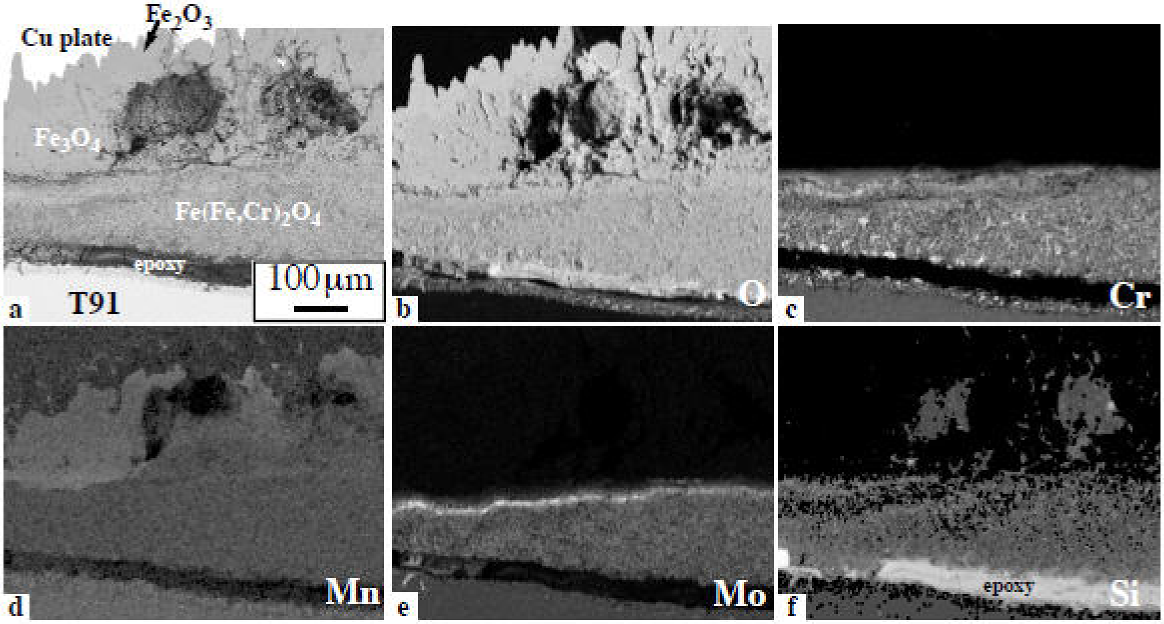

Figure 3-5
EPMA secondary electron image of the reaction product formed on Grade 91 after 10 hours at 1050°C (1922°F) in dry air and elemental maps from (a) showing (b) O, (c) Cr, (d) Mn, (e) Mo, and (f) Si. In the gray-scale maps, black indicates no detection, and lighter areas indicate higher concentration.

Figure 3-5 also shows the multilayered nature of the thick, porous, and brittle oxide formed on Grade 91 at high temperatures. Labels in Figure 3-5a identify the three layers in the oxide formed after 10 hours at 1050°C (1922°F) in air—a relatively thin, dense layer of Fe_2O_3 at the gas interface, a porous Fe_3O_4 beneath, and a mixture of Fe_3O_4 and $FeCr_2O_4$ adjacent to the metal substrate. (These phases were confirmed by XRD and EPMA.) The low Cr level in the outer layer is indicated by the lack of signal in the upper part of Figure 3-5c. The maps show no clear Mn enrichment (Figure 3-5d) and a weak Mo enrichment near the Fe_3O_4-$Fe(Fe,Cr)_2O_4$ interface (Figure 3-5e). The Si map is confounded by the presence of epoxy mounting material near part of the metal-scale interface and by polishing media in some of the large porosity embedded during the polishing process. Figure 3-6 shows a plan view of the oxide formed after 1 hour at 1050°C (1922°F) before sectioning to show the outward-growing outer layer (Figure 3-6a) and the fine-grained (possibly porous) inner layer in areas where the outer oxide has spalled (Figure 3-6b).

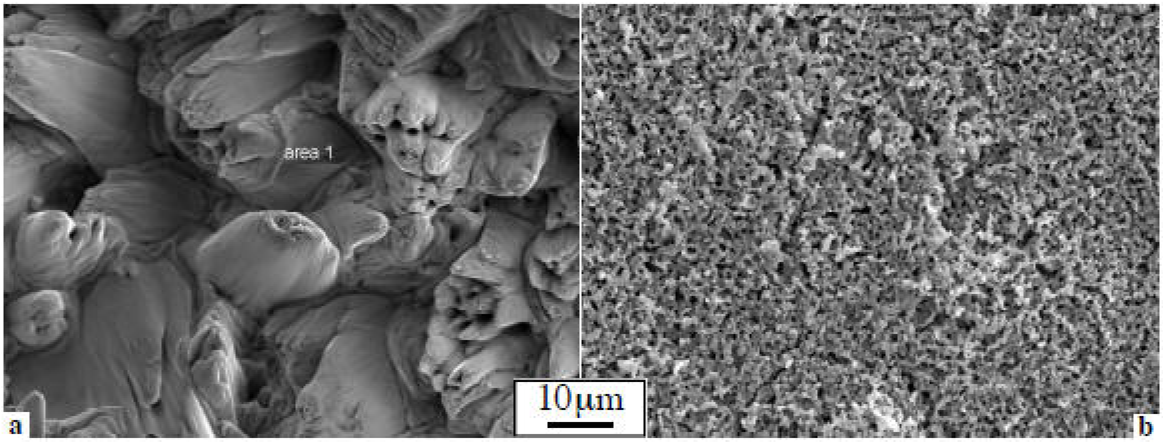

Figure 3-6
SEM secondary electron plan-view images of the scale formed on Grade 91 after 1 hour at 1050°C (1922°F) in dry air: (a) shows the morphology of the outermost Fe_2O_3 scale, and (b) shows the more porous, finer grained inner oxide in areas where the outer scale has spalled

Finally, Figure 3-7 shows EPMA concentration profiles from oxides formed at 1050°C (1922°F). In the area analyzed after 1 hour, the outer oxide has spalled (Figure 3-7a). The analysis of the inner layer shows a Cr level similar to the alloy and little enrichment of Mo or Mn (Figure 3-7b). (The higher Si levels in the oxide could be embedded polishing media or an enrichment.) The area analyzed after 10 hours (the same area that was mapped in Figure 3-5) has the complete oxide (Figure 3-7c). The inner layer has a composition similar to that after 1 hour (Figure 3-7d). The outermost oxide contained ~57at. % O, slightly lower than the 60% expected in Fe_2O_3. The Fe_3O_4 inner layer contained 52% to 55% O, with very little Cr detected but a constant 0.3% Mn content throughout the layer (arrow in Figure 3-7d).

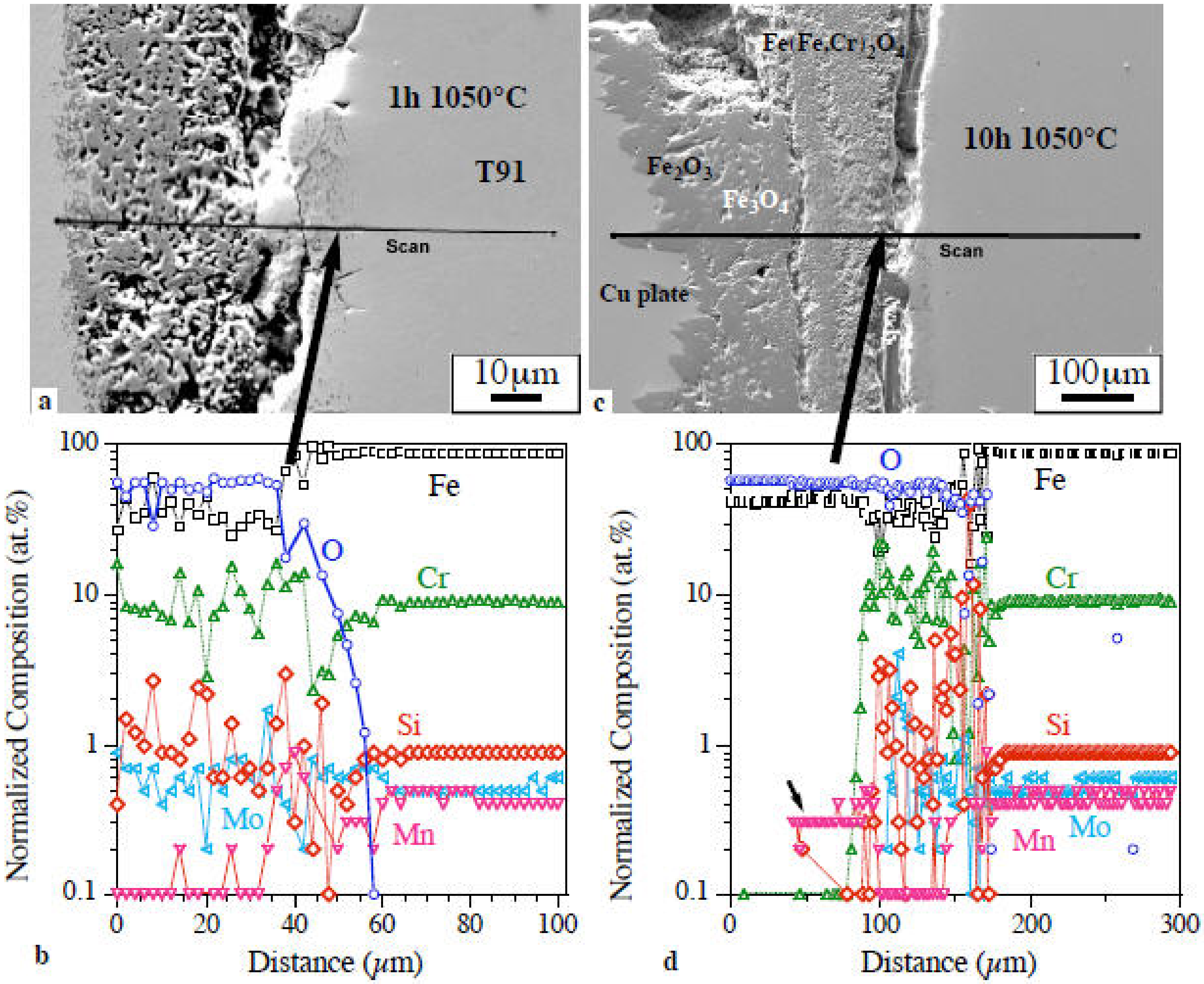

Figure 3-7
EPMA secondary electron images (a, c) and line profile composition information (b, d) for oxides formed on Grade 91 in dry air at 1050°C (1922°F) for 1 hour (a, b) and 10 hours (c, d)

Figure 3-8 shows the oxide formed at 850°C–950°C (1562°F–1742°F). As observed in the kinetic data, the oxide growth rates are high in this temperature range. The oxides formed at 950°C (1742°F) are very similar to those formed at higher temperatures (Figures 3-8a and 3-8b). However, as seen in Figures 3-8c and 3-8e, the scale formed after exposure for 1 hour at 900°C (1652°F) and 850°C (1562°F), respectively, is relatively thin compared with higher temperatures. At these temperatures, Grade 91 transitions from somewhat protective behavior to rapid oxidation due to the formation of Fe-rich oxide after a 10-hour exposure. This transition is particularly easy to see at 850°C (1562°F) where small oxide nodules formed after 1 hour (arrows in Figure 3-8e). These nodules grew during a 10-hour exposure to form the multilayered thick scale observed at all of the higher temperatures (Figure 3-8f).

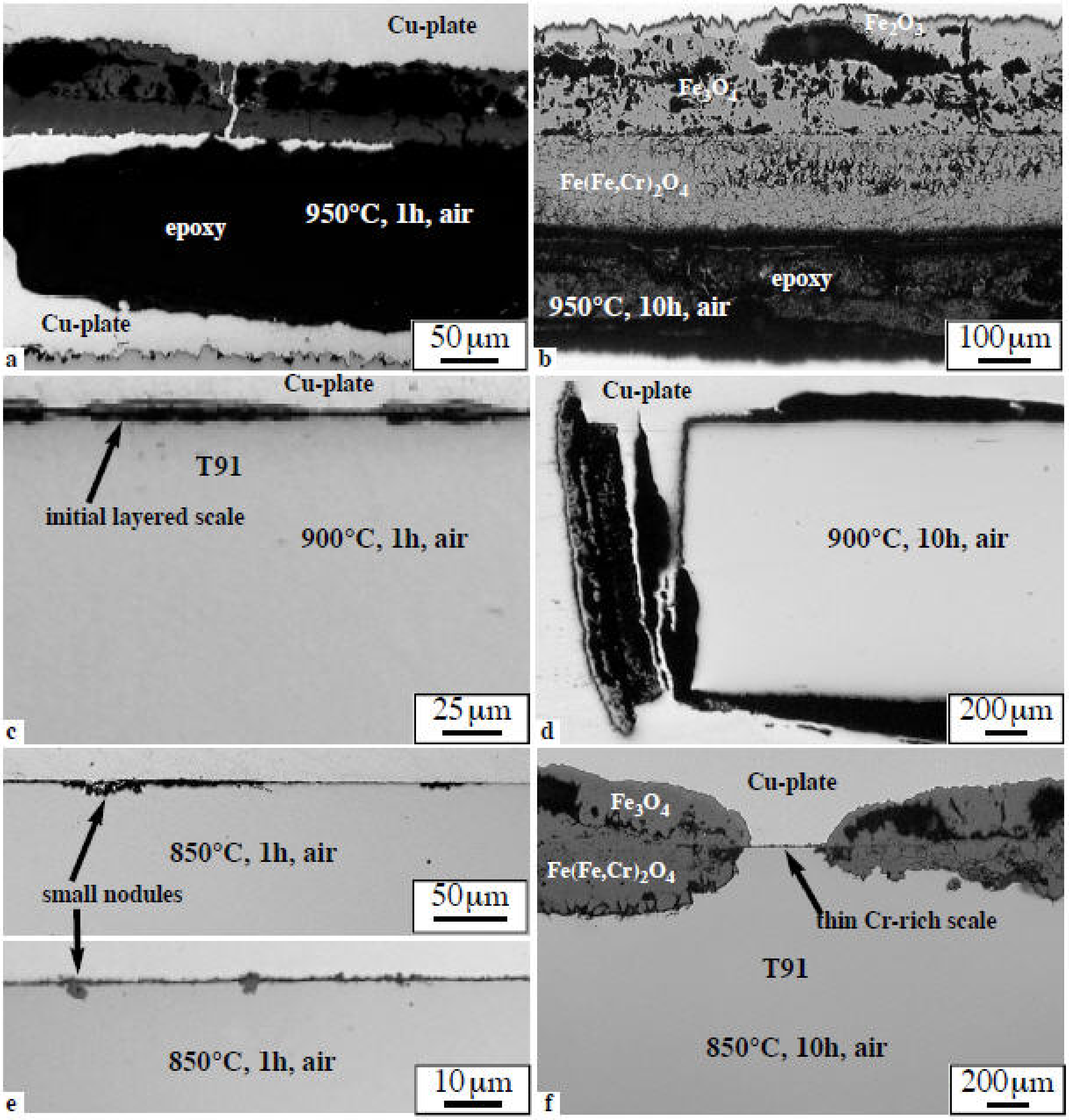

Figure 3-8
Light microscopy of polished cross sections of Grade 91 oxidized in dry air for (a) 1 hour at 950°C (1742°F), (b) 10 hours at 950°C (1742°F), (c) 1 hour at 900°C (1652°F), (d) 10 hours at 900°C (1652°F), (e) 1 hour at 850°C (1562°F; two areas), and (f) 10 hours at 850°C (1562°F)

A region similar to Figure 3-8f is further characterized by EPMA in Figure 3-9.

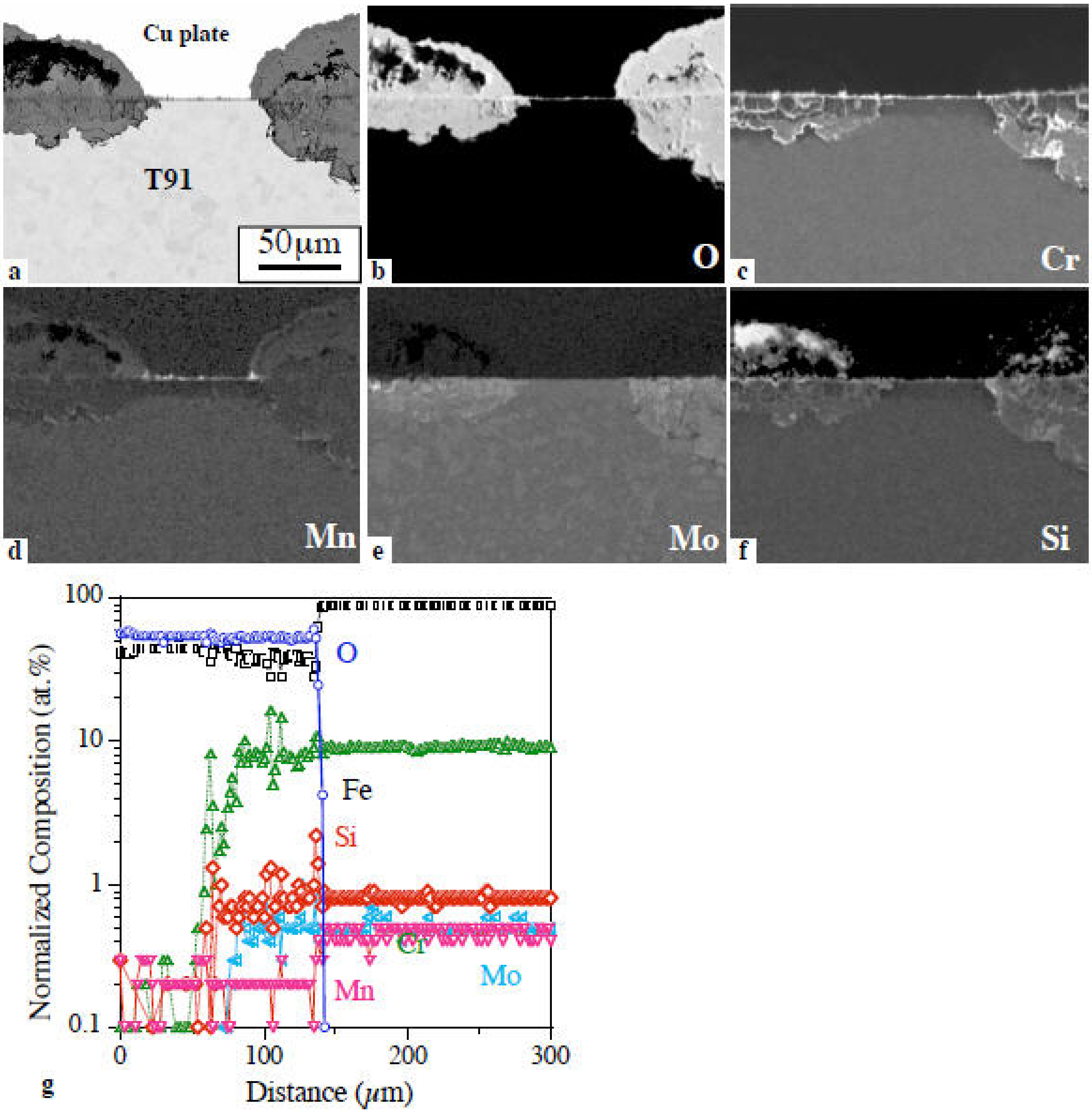

Figure 3-9
(a) EPMA secondary electron image of the reaction product formed on Grade 91 after 10 hours at 850°C (1562°F) in dry air and elemental maps from (a) showing (b) O, (c) Cr, (d) Mn, (e) Mo, and (f) Si: (g) Shows a normalized composition profile across one of the oxide modules from the gas interface into the metal

Typical of Fe-Cr alloys in the transition between protective and nonprotective behavior, there are regions of thin oxide remaining that are rich in Cr, Mn, and Si (center of maps in Figure 3-9). The nodules are similar in structure and composition to the thick scales formed at higher temperatures. A nodule composition profile is shown in Figure 3-9g and indicates that the nodule has the familiar three-layer structure of Fe_2O_3/Fe_3O_4/$Fe(Fe,Cr)_2O_3$.

The scales formed at 750°C–800°C (1382°F–1472°F) in dry air are thin and protective. They are similar to the remaining thin oxide in Figure 3-9. Figure 3-10 shows cross sections of the scales formed at 750° (1382°F) and 800°C (1472°F). Figure 3-11 gives an example of the gas-side oxide morphology with a few larger oxide nodules rich in Mn (arrows). Figure 3-12 shows EPMA composition profiles from the thin protective oxides and underlying metal for Grade 91 specimens exposed at 750°C (1382°F) and 800°C (1472°F). These composition profiles show the protective oxides to be rich in Cr and Mn, with a very minor Cr and Mn depletion in the metal beneath the scale at 750°C (1382°F; Figure 3-12b) and a slightly greater depletion at 800°C (1472°F; Figure 3-12d), in agreement with expectations. At higher temperatures, this depletion leads to Fe-rich oxide formation and internal oxidation of the Cr.

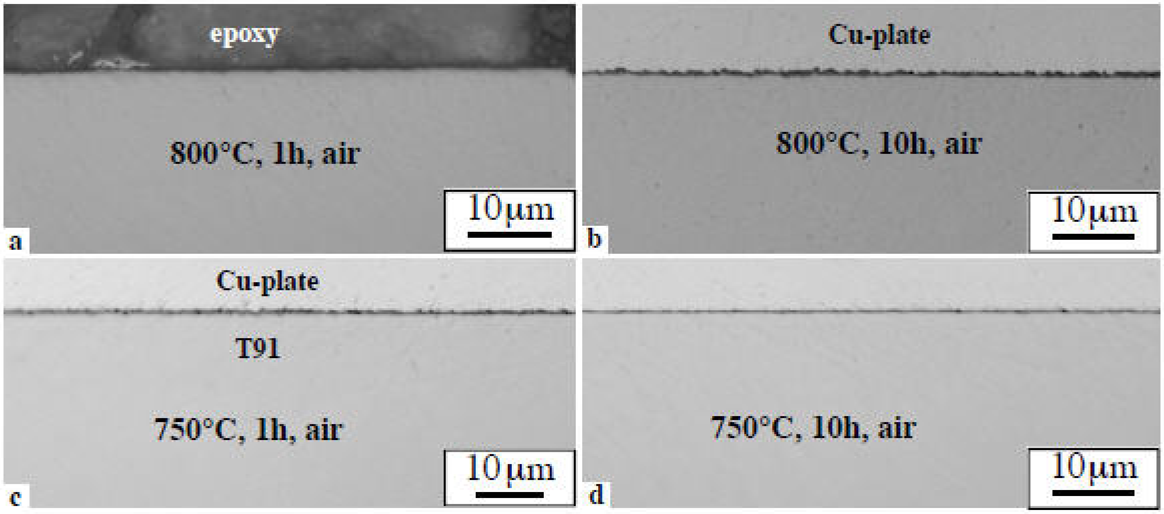

Figure 3-10
Light microscopy of polished cross sections of Grade 91 oxidized in dry air for (a) 1 hour at 800°C (1472°F), (b) 10 hours at 800°C (1472°F), (c) 1 hour at 750°C (1382°F), and (d) 10 hours at 750°C (1382°F)

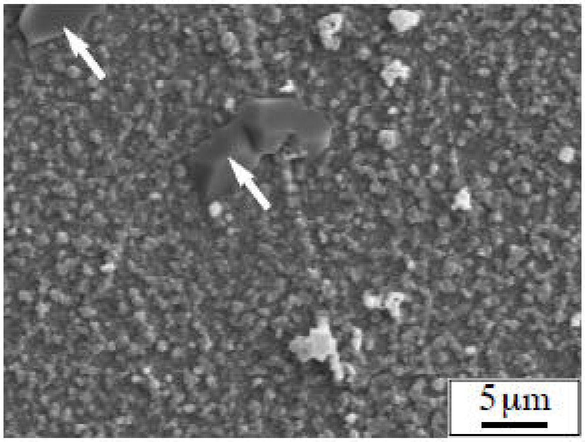

Figure 3-11
SEM secondary electron plan-view image of the scale formed on Grade 91 after 10 hours at 750°C (1382°F). Arrows mark Mn-rich oxides on the surface.

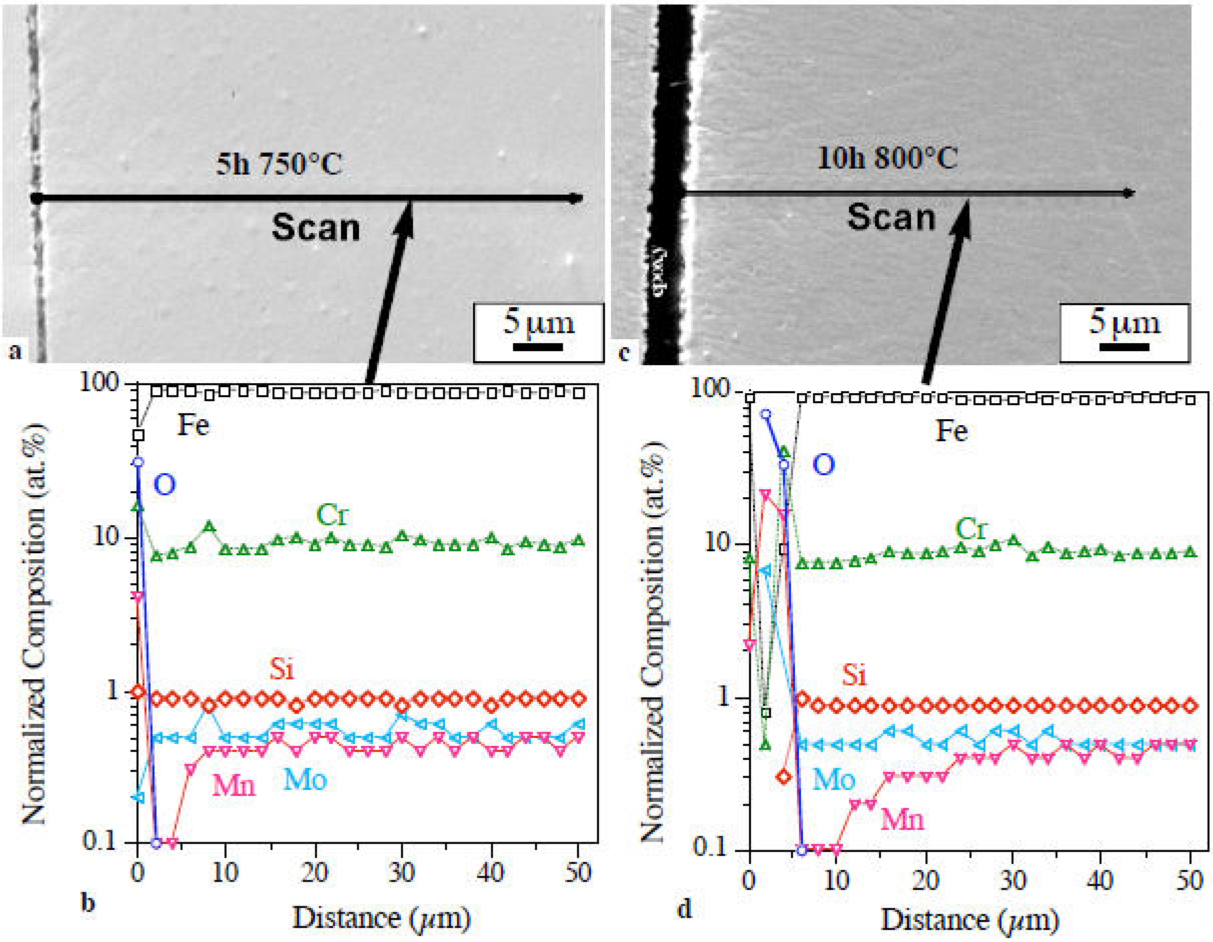

Figure 3-12
EPMA secondary electron images (a, c) and line profile composition information (b, d) for oxides formed on Grade 91 in dry air for (a, b) 5 hours at 750°C (1382°F) and (c, d) 10 hours at 800°C (1472°F)

Effect of Simulated Two-Stage Heat Treatment

Figure 3-13 shows a polished cross section of a Grade 91 specimen given a two-stage oxidation treatment of 1 hour at 1050°C (1922°F) followed by 2 hours at 750°C (1382°F; simulating normalizing and tempering treatments). The specimen was cooled to room temperature between the exposures. Spallation of the thick oxide formed at 1050°C (1922°F) made measuring the mass change by TGA very difficult. A large mass loss due to scale spallation was observed for the second stage at 750°C (1382°F). The resulting oxide after the 750°C (1382°F) oxidation was a thicker oxide than what was formed after only 2 hours at 750°C (1382°F). This difference was attributed to oxidation of the surface metal where some of the Cr was tied up as internal oxide after the 1 hour at 1050°C (1922°F) exposure (Figure 3-4c). The metal near the surface was effectively depleted in Cr and formed a thicker, Fe-rich oxide rather than the thin Cr- and Mn-rich oxide formed on Grade 91. Some areas formed an even thicker mixed oxide-metal surface layer (Figure 3-13). This structure also is attributed to the internal oxidation during the 1050°C (1922°F) exposure.

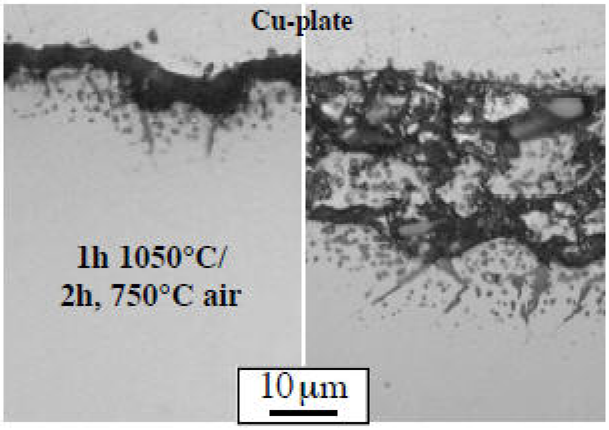

Figure 3-13
Light microscopy of a polished cross section of Grade 91 oxidized in dry air for 1 hour at 1050°C (1922°F) cooled to room temperature and then oxidized for 2 hours at 750°C (1382°F). The two regions showed different oxide structures.

Oxidation in Steam

Figure 3-14 shows the mass change for Grade 91 specimens exposed in 500-hour cycles at 600°C (1112°F) in steam at 17 bar (247 psi). Specimens were exposed with and without pre-oxidation in air to simulate the alloy heat treatments. Many of the specimens were stopped after a 1000-hour exposure, while the rest were exposed for 2000 hours. The three as-polished specimens without pre-oxidation gained mass with a parabolic rate. The plan view of the scale formed on one of these specimens is shown in Figure 3-15a. The cross section of a similar Grade 91 specimen is shown in Figure 3-16a. In steam, the thick duplex oxide and internal oxidation form at a much lower temperature than in air because of differences in the oxidation mechanism in the presence of H_2O.

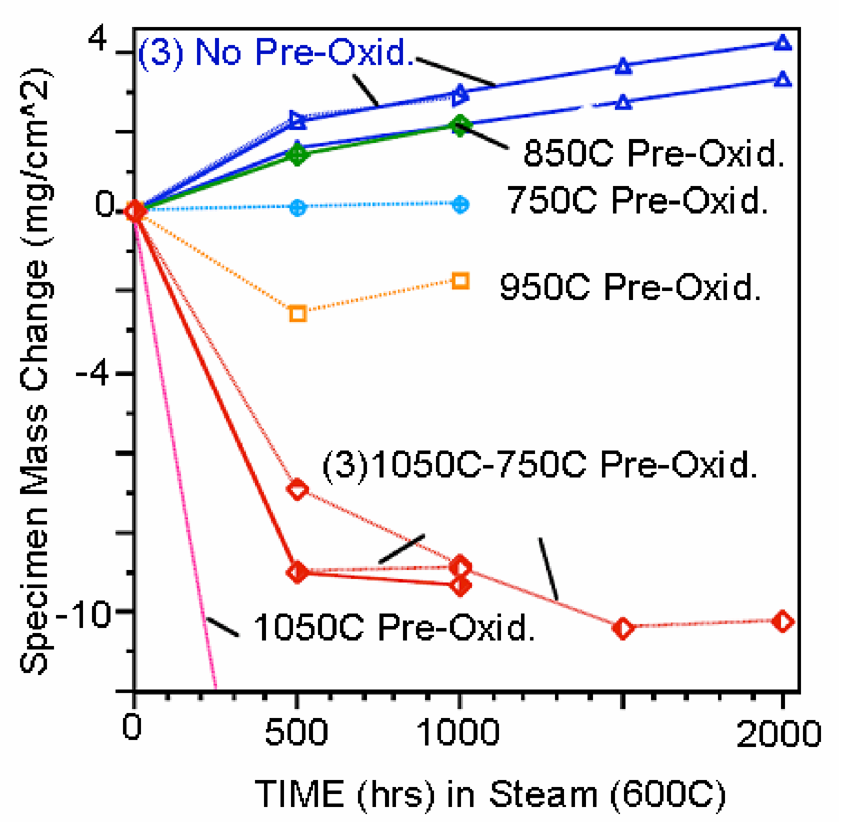

Figure 3-14
Mass gain of Grade 91 specimens exposed in 500-hour cycles at 600°C (1112°F) in steam at 17 bar (247 psi). Three specimens were exposed with a polished-surface finish, and the other specimens had pre-oxidation for 1 hour at temperatures ranging from 850°C–1050°C (1562°F–1922°F) or 2 hours at 750°C (1382°F). Most of the specimens were stopped after 1000 hours, with a few continuing to 2000 hours.

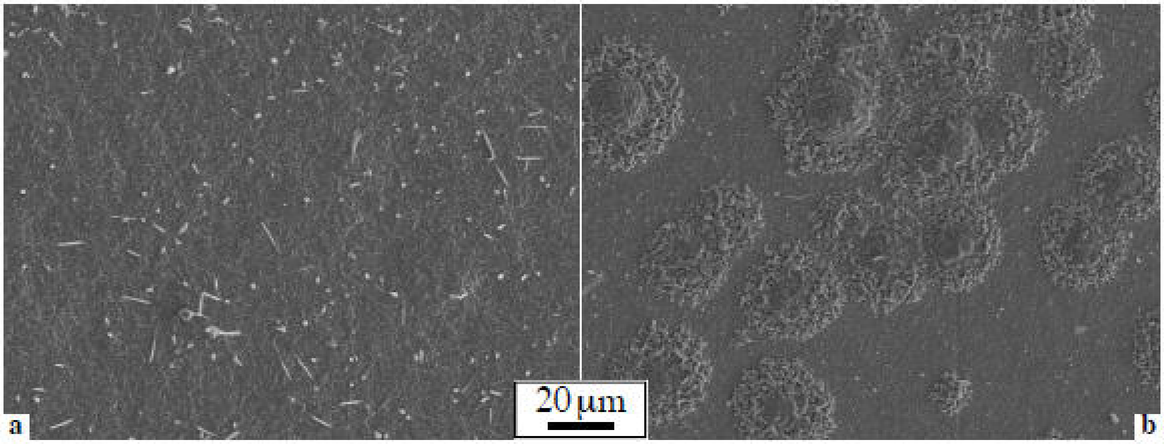

Figure 3-15
SEM secondary electron plan-view images of Grade 91 specimens exposed at 600°C (1112°F) in steam at 17 bar (247 psi): (a) as-polished and (b) pre-oxidized for 2 hours at 750°C (1382°F)

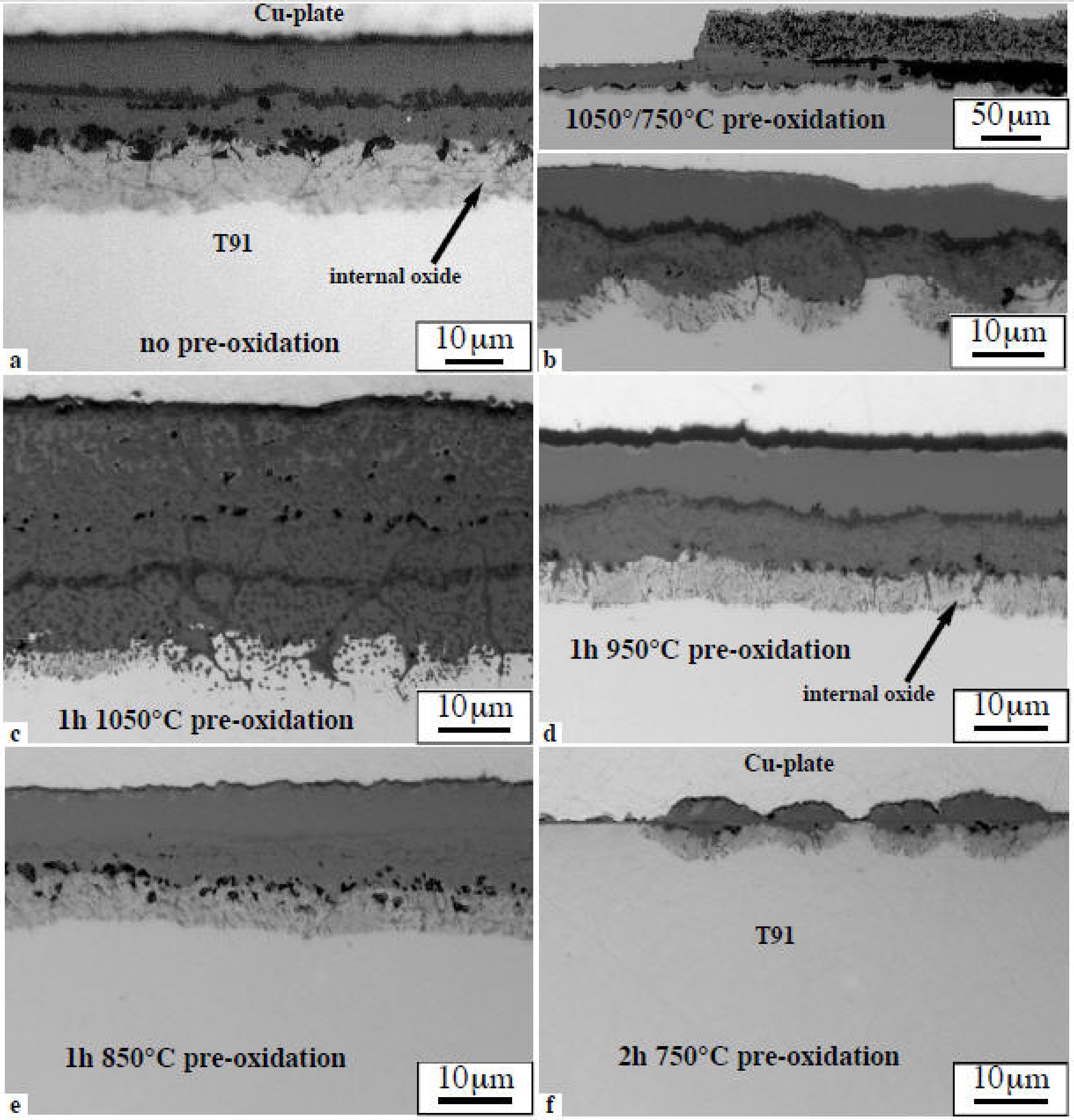

Figure 3-16
Light microscopy of polished Grade 91 specimens exposed for 1000 hours at 600°C (1112°F) in steam at 17 bar (247 psi): (a) no pre-oxidation, (b) pre-oxidation for 1 hour at 1050°C (1922°F) and 2 hours at 750°C (1382°F; two magnifications), (c) pre-oxidation for 1 hour at 1050°C (1922°F), (d) pre-oxidation for 1 hour at 950°C (1742°F), (e) pre-oxidation for 1 hour at 850°C (1562°F), and (f) pre-oxidation for 2 hours at 750°C (1382°F)

With air pre-oxidation for 1 hour at 1050°C (1922°F; simulating only the normalization treatment), a very large mass loss was measured (23 mg/cm^2) during the subsequent steam exposure due to spallation of large flakes of the thick oxide formed during pre-oxidation. Similarly, the three specimens pre-oxidized for 1 hour at 1050°C (1922°F) and 2 hours at 750°C (1382°F; simulating normalization and tempering treatments) all showed a large mass loss due to scale spallation (Figure 3-14). These observations suggest that the thick oxides formed during the normalizing heat treatment in air will likely spall after exposure to steam.

The specimens pre-oxidized at lower temperatures showed lower mass changes. The pre-oxidation at 950°C (1742°F) showed a lower mass loss due to the thinner scale formed at this temperature, while the 850°C (1562°F) pre-oxidation appeared to have no net effect on the mass change (Figure 3-16). The most noteworthy observation was made with the 750°C (1382°F) pre-oxidation where the mass gain was lower than for the specimens that were not pre-oxidized. A plan view of the oxide formed on that specimen is shown in Figure 3-15b and indicates the formation of oxide nodules on the surface. In the cross section, the scale was thinner than that formed in steam without pre-oxidation (Figure 3-16f). However, the formation of the nodules suggested that the benefit of 750°C (1382°F) pre-oxidation will be short-lived and lead to little or no long-term effect on steam oxidation behavior. As the Cr-rich pre-oxidation layer is breached, a thicker oxide will likely form and will be very similar to the alloy without pre-oxidation. Figure 3-16 shows cross sections of the other pre-oxidized specimens exposed for 1000 hours at 600°C (1112°F) in steam at 17 bar (247 psi). The reaction products generally were similar to those formed on the Grade 91 specimen without pre-oxidation. The same Fe_2O_3, Fe_3O_4, and $FeCr_2O_4$ phases were identified after exposure in steam as those that were formed in dry air. However, no EPMA characterization has been performed on the specimens exposed in steam.

Figure 3-17 shows polished cross sections from specimens exposed for 2000 hours in steam at 17 bar (247 psi) at 600°C (1112°F). There was some difference seen in the scale formed with and without the two-stage pre-oxidation at 1050° (1922°F)/750°C (1382°F). While both had a two-layer scale, the pre-oxidized specimen was less regular and appeared to have less internal oxidation compared with the specimen without pre-oxidation. Compared with similar specimens exposed for 1000 hours (Figures 3-16a and 3-16b), each of the layers appeared to increase in thickness with increased exposure time. The as-polished specimen in Figure 3-17a appeared to be forming a thin layer of Fe_2O_3 at the gas interface. However, further characterization to determine changes in chemical composition was not conducted on these specimens. The oxides were consistent with the mass gains for these specimens in Figure 3-14. The large mass loss for the pre-oxidized specimen is associated with spallation of the initial air-formed oxide.

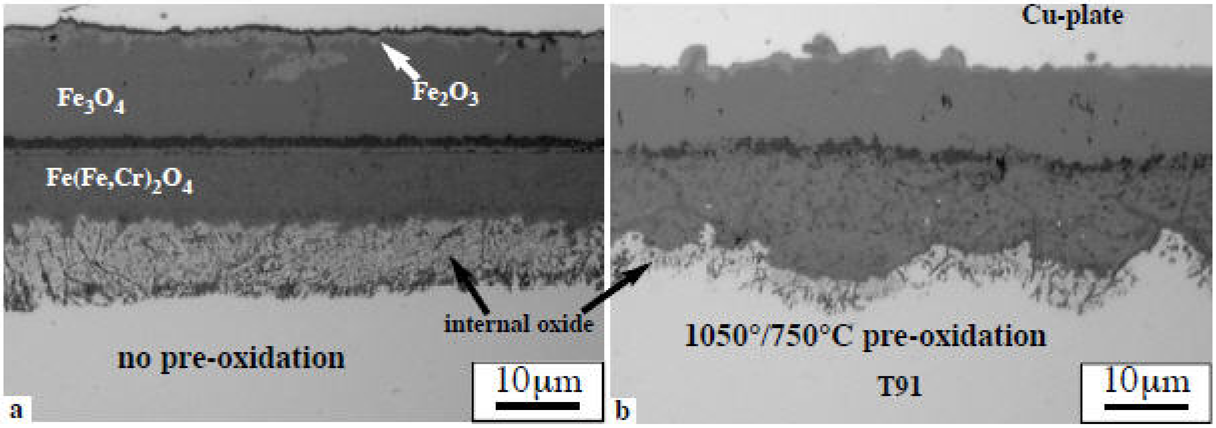

Figure 3-17
Light microscopy of polished Grade 91 specimens exposed for 2000 hours at 600°C (1112°F) in steam at 17 bar (247 psi): (a) no pre-oxidation and (b) pre-oxidation for 1 hour at 1050°C (1922°F) and 2 hours at 750°C (1382°F)

4
SUMMARY

Specimens of Grade 91 were exposed at 750°C (1382°F) to 1050°C (1922°F) in dry air at 1 bar (14 psi) and at 600°C (1112°F) in steam at 17 bar (247 psi) for up to 2,000 hours with and without pre-oxidation in air to gain a better understanding of the rates of oxidation and reaction products likely to result from the typical heat treatment required for this alloy. Very rapid oxidation was observed for Grade 91 in air at temperatures above 800°C (1472°F). Above 950°C (1742°F), further temperature increases did not significantly raise the very rapid oxidation rate. The external oxides or scales were characterized by SEM, XRD, EPMA, and metallographic cross sections to determine the scale thickness and types of oxides formed. The primary effect of pre-oxidation in air on subsequent steam exposure at 600°C (1112°F) appeared to be the spallation of the thicker preformed oxides. Because of the scale spallation, it was difficult to determine the rate of oxidation of the pre-oxidized Grade 91 specimens in steam. In general, pre-oxidation had little effect on the oxide phases formed in steam except for pre-oxidation at 750°C (1382°F) where the thin Cr-rich scale formed in air appeared to temporarily inhibit the formation of a thick, Fe-rich scale. However, the formation of Fe-rich oxide nodules on the 750°C (1382°F) pre-oxidized specimen after 1000 hours in steam at 600°C (1112°F) suggested that the benefit would be short-lived. The data presented in this report may provide a basis for comparing field-heat treated Grade 91 welds to determine the heat treatment temperature based on the oxide thickness. The source of the thick oxide (normalization or subsequent growth in steam) may be identified by the internal oxidation. However, this identification needs to be verified by examining field-exposed tubes.

Overall, a normalizing (1 hour at 1050°C [1922°F]) and tempering (2 hours at 750°C [1382°F]) heat treatment of Grade 91 in air produces oxide scales whose thickness is sufficient enough (and/or inherently non-adherent) that they will be lost by spallation when those surfaces are exposed to steam. The techniques used in this study did not permit a reliable estimation of the amount or size of the spalled oxide. Nevertheless, such scale spallation carries the potential for problems in service. Minimizing scale formation by controlling the environment or removing the pre-oxidized scale before exposure to steam appear to be desirable strategies. These strategies would be easier to implement for shop-fabricated parts rather than field repairs. In the field, perhaps reducing the normalizing temperature to ~1000°C (~1832°F) and minimizing the normalizing time could reduce the amount of oxidation.

5

RECOMMENDATIONS FOR ADDITIONAL RESEARCH

Based on the research described in this report, the following recommendations are made:

- Comparison with field-exposed T91 tubes to evaluate oxide morphologies and internal oxidation zones.
- Further exposures in air followed by longer exposures in steam to quantify the amount of scale (size of spall and type of oxide) lost by spallation in steam. Exposure of multiple specimens for each condition and the use of a combination of posttest characterization techniques would provide the best approach for generating quantitative information. The exposure conditions would be selected to represent specific scenarios with realistic heat-treatment schedules and operating practices.
- Similar exposures involving removing the air-formed oxide layer before exposure to steam. The aim of this experiment would be to verify the scale-removal strategy and determine any additional effects of the removal procedure on scale growth and adhesion.
- Exposure of miniature tensile-creep specimens (25 mm long; 2x2-mm gage) to determine the effect of exposure and heat treatment on the alloy mechanical properties.

Export Control Restrictions

Access to and use of EPRI Intellectual Property is granted with the specific understanding and requirement that responsibility for ensuring full compliance with all applicable U.S. and foreign export laws and regulations is being undertaken by you and your company. This includes an obligation to ensure that any individual receiving access hereunder who is not a U.S. citizen or permanent U.S. resident is permitted access under applicable U.S. and foreign export laws and regulations. In the event you are uncertain whether you or your company may lawfully obtain access to this EPRI Intellectual Property, you acknowledge that it is your obligation to consult with your company's legal counsel to determine whether this access is lawful. Although EPRI may make available on a case-by-case basis an informal assessment of the applicable U.S. export classification for specific EPRI Intellectual Property, you and your company acknowledge that this assessment is solely for informational purposes and not for reliance purposes. You and your company acknowledge that it is still the obligation of you and your company to make your own assessment of the applicable U.S. export classification and ensure compliance accordingly. You and your company understand and acknowledge your obligations to make a prompt report to EPRI and the appropriate authorities regarding any access to or use of EPRI Intellectual Property hereunder that may be in violation of applicable U.S. or foreign export laws or regulations.

The Electric Power Research Institute Inc., (EPRI, www.epri.com) conducts research and development relating to the generation, delivery and use of electricity for the benefit of the public. An independent, nonprofit organization, EPRI brings together its scientists and engineers as well as experts from academia and industry to help address challenges in electricity, including reliability, efficiency, health, safety and the environment. EPRI also provides technology, policy and economic analyses to drive long-range research and development planning, and supports research in emerging technologies. EPRI's members represent more than 90 percent of the electricity generated and delivered in the United States, and international participation extends to 40 countries. EPRI's principal offices and laboratories are located in Palo Alto, Calif.; Charlotte, N.C.; Knoxville, Tenn.; and Lenox, Mass.

Together…Shaping the Future of Electricity

© 2009 Electric Power Research Institute (EPRI), Inc. All rights reserved. Electric Power Research Institute, EPRI, and TOGETHER…SHAPING THE FUTURE OF ELECTRICITY are registered service marks of the Electric Power Research Institute, Inc.

1017470